

The Effect of Chemical Reaction on Heat and Mass Transfer MHD flow with Ag, TiO₂ and Cu Water Nanofluids over a Semi Infinite Surface

Dharmaiah.G^{1*}, Prakash.J², Balamurugan.K.S³ and Vedavathi.N⁴

^{1}Department of Mathematics, Narasaraopeta Engineering College, Narsaraopet, Andhra Pradesh, India.*

²Department of Mathematics, University of Botswana, Botswana.

³Department of Mathematics, RVR & JC College of Engineering, Guntur, Andhra Pradesh, India.

⁴Department of Mathematics, K.L. University, Vaddeswaram, Guntur, Andhra Pradesh, India.

Abstract

In this article, we have examined a Chemical reaction and Radiation Absorption on MHD free convective heat and mass transfer flow of a nanofluid bounded by a semi infinite flat plate with Diffusion thermo(Dufour). The numerical solutions of the boundary layer equations are assumed of oscillatory type. Three types of nano fluids are used namely Ag-water nano fluid, TiO₂-water nanofluid and Cu-water nanofluid, with the moving plate with constant velocity U_0 . Temperature and concentration are assumed to be fluctuating with time harmonically from a constant mean at the plate surface. We have solved the model equations using two-term perturbation technique. Comprehensive numerical computations are conducted for various values of the parameters describe the flow characteristics and results are illustrated graphically. Skin friction coefficient, wall heat transfer rate and wall mass transfer rate presented in table form.

Keywords: Nanofluids, Chemical reaction, Boundary layer flow, Radiation Absorption, MHD, Heat and Mass Transfer.

MSC 2010: 76M20, 76N20, 76W05, 80A20, 35Q35.

Nomenclature

u' - velocity component along x-axis, v' - velocity component along y-axis, ϕ - the solid volume fraction of the nanoparticles, K_{nf} - the thermal conductivity of the base fluid, K_s - the thermal conductivity of the solid, β_f - the coefficient of the thermal expansion of the fluid, β_c - the coefficient of the thermal expansion of the solid, ρ_f - the density of the fluid fraction, ρ_c - the density of the solid fraction, β_{nf} - the coefficient of thermal expansion of nanofluid, σ - the electric conductivity of the fluid, ρ_{nf} - the density of the nanofluid, μ_{nf} - the viscosity of nanofluid, $(\rho C_p)_{nf}$ - the heat capacitance of nanofluid, g - the acceleration due to gravity, K' - the permeability porous medium, T' - the temperature of the nanofluid, Q - the temperature dependent volumetric rate of the heat source, α_{nf} - the thermal diffusivity of the nanofluid, U_0 - uniform reference velocity, ε - perturbation parameter, u - velocity components in the x-axis, v - velocity components in the y-axis, C - Nanoparticle concentration, f - Fluid, w - condition at wall, ∞ - Ambient Condition, T'_w - Temperature at the surface, T'_∞ - Ambient temperature, C_f - skin friction coefficient, C_p - specific heat at constant pressure, C'_∞ - Ambient concentration, nf - nanofluid, σ - electrical conductivity of the fluid.

1. INTRODUCTION

Convective heat transfer in nano fluids is a topic of major contemporary interest both in sciences and in engineering. In many chemical engineering processes, a chemical reaction between a foreign mass and the fluid does occur. These processes take place in numerous industrial applications, such as the polymer production, the manufacturing of ceramics or glassware, food processing, etc. The study of heat and mass transfer with chemical reaction in the presence nanofluids is of immense realistic significance to engineers and scientists because of its almost universal incidence in many branches of science and engineering. This phenomenon plays an important role in chemical industry, power and cooling industry for drying, chemical vapor deposition on surfaces, cooling of nuclear reactors and petroleum industries.

Nanofluids with or without the presence of magnetic field have many applications in the industries since materials of nanometer size have unique chemical and physical

properties with regard to sundry applications of nano fluids, the cooling applications of nanofluids include silicon mirror cooling, electronics cooling, vehicle cooling, transformer cooling, etc. This study is more important in industries such as hot rolling, melt spinning, extrusion, glass fiber production, wire drawing, manufacture of plastic and rubber sheets, etc. The research on nanofluids is gaining a lot of attention in recent years. A nanofluid is a new class of heat transfer fluids that contain a base fluid and nanoparticles. The use of additives is a technique applied to enhance the heat transfer performance of base fluids. The thermal conductivity of ordinary heat transfer fluids is not adequate to meet today's cooling rate requirements. Nanofluids have been shown to increase the thermal conductivity and convective heat transfer performance of the base liquids. Nanofluids are suspensions of submicronic solid particles (nanoparticles) in common fluids. Nanofluids are suspensions of metallic, non-metallic or polymeric nano-sized powders in a base liquid which are used to increase the heat transfer rate in various applications. In recent years, the concept of nanofluid has been proposed as a route for increasing the performance of heat transfer liquids. Due to the increasing importance of nanofluids, there is a large amount of literature on convective heat transport in nanofluids problems. Nanofluid is described as a fluid containing nanometer-sized particles, called nanoparticles within the length scale of 1-100 nm diameter and 5% volume fraction of nanoparticles. These fluids are suspended in engineering colloidal system of nanoparticles in a base fluid. As oil, ethylene glycol and water are poor heat transfer fluids, because they have low thermal conductivities or low heat transfer properties. Solar energy perhaps has a reasonable solution with the hourly solar flux incident on the earth's surface being greater than all the consumption of energy in a year. Solar energy is also known as a best source of renewable energy with the minimal environmental impact. Power tower solar collectors are more effective through the use of nanofluid as a working fluid. Recently, the nanofluids in view of their enhanced thermal characteristics have been attracted by the scientists and engineers. It is known well established fact that the nanofluids improve the heat transfer performance of many engineering applications. The theory of nanofluid is first introduced by Choi (1995) and has been a field of active research area for about two decades. Choi has suggested the injection of nano-size particles into regular fluids, such as water and oil. He has proved experimentally that the injection of these particles improves the thermal conductivity of the fluid. This conclusion has opened the way to use these new fluids in chemical engineering, mechanical engineering, medicine, and many other fields. This fluid is a suspension of a nanometer size solid particles and fibres in a convectional base fluid. In recent years, the concept of a nanofluid has been proposed as a route for enhancing the performance of the heat transfer rates in the liquids. Materials, with sizes of nanometers possess unique physical and chemical properties.

R.V.M.S.S Kiran kumar et al.,[1] have been studied in the direction of the temperature and concentration are assumed to be fluctuating with time.

G.Venkataramanaiah et al.,[2] have been explained the nano particle effect on MHD boundary layer flow of Williamson fluid over a stretching sheet. Dodda Ramya et al.,[3] have been investigated the steady two-dimensional flow of a viscous nano-fluid of MHD flow for the boundary layer flow. P.Srinivasulu et al.,[4] have been presented heat transfer and MHD thermal boundary layer flow over a non linear stretching sheet with radiation and uniform heat source for different types of Nano-fluids. Fekry M Hady et al., [5] have been discussed the steady state thermal boundary layer flow with nonlinearly stretching sheet in Nano-fluids. Sandeep Naramgiri et al., [6] have been illustrated the buoyancy-driven MHD mixed convection stagnation-point flow, heat and mass transfer of a fluid over a non-isothermal stretching sheet. Nader Y Abd Elazem et al., [7] have been discussed influence of radiation for steady state MHD Nano fluid flows. Nageeb A Haroun et al., [8] have been numerated Dufour and Soret effects along with viscous dissipation. Eshetu Haile et al., [9] have been presented on heat and mass transfer characteristics of a moving plate of nanofluids. P.V.Satyanarayana et al., [10] have been considered chemical reaction and heat source effects on unsteady MHD free convection heat and mass transfer of a nano fluid flow past a semi-infinite flat plate in a rotating system. Mohammad Mehdi Keshtekar et al., [11] have been investigated mixed convection MHD flow of nano fluid over a nonlinear stretching sheet with variable magnetic field. M.J.Uddin et al.,[12] have been examined under Navier velocity slip, Newtonian heating and passively controlled wall boundary conditions of a nanofluid past a radiating sheet. Mohamed Abdel-wahed et al.,[13] have been analysed the MHD boundary layer with convective boundary conditions over a flatness-moving surface taking the nano particles Brownian motion. K.Vendabai et al., [14] have been studied a nanofluid over a stretching surface with variable transport properties. D.R.V.S.R.Sastry [15] has been noticed that inclusion of the magnetic field parameter on the flow increased the temperature and decreased the velocity profiles concerned. S.A.Shehzad et al [16] have been developed convective mass condition at the surface in flow analysis with nano particles. Imran Anwar et al., [17] have been considered on a nanofluid with the simultaneous heat and mass transfer when the MHD stagnation point flow of a nanofluid porous stretching sheet. M.Turkyilmazoglu [18] has been performed the time dependent flow past an impulsively started vertical infinite isothermal plate in a viscous electrically conducting natural convective incompressible nanofluid. G.S.Seth et al.,[19] have been obtained in their results rotation trends to retard fluid flow in the primary flow direction where as it has a reverse effect on the fluid flow in the secondary flow direction. Wubshet Ibrahim et al.,[20] have been considered slip boundary conditions to the boundary layer flow and heat transfer analysis of nanofluid.

In the present study, we investigate the flow and heat transfer phenomena over a semi infinite plate with velocity, temperature and concentration at the boundary conditions. The problem is solved by perturbation technique. The effects of different flow

parameters on the velocity, temperature and concentration profiles were sketched and analyzed. In addition, the local skin-friction, the heat and mass transfer rates were examined.

2. ANALYSIS OF THE FLOW OF THE PROBLEM

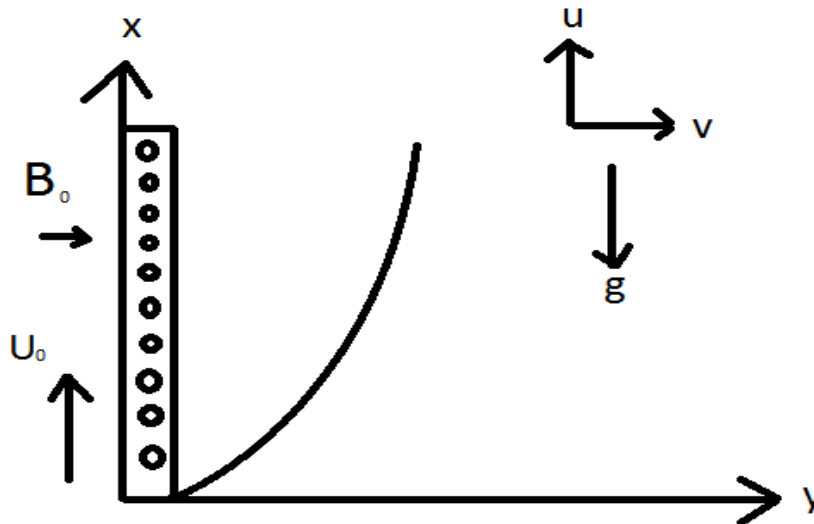


Figure 1. Flow model diagram

An unsteady natural conventional flow of a nanofluid past a vertical permeable semi-infinite moving plate with constant heat source is considered. The physical model of the fluid flow is shown in Figure.1. The flow is assumed to be in the x -direction which is taken along the plate and y -direction is normal to it. A uniform external field of strength B_0 is taken to be acting along the y -direction. It is assumed that the induced magnetic field and the external electric field due to polarization of charges are negligible. The plate and the fluid are the same temperature T_∞' and concentration C_∞' in a stationary condition, when $t \geq 0$, the temperature and concentration at the plate fluctuate with time harmonically from a constant mean. The fluid is a water based nanofluid containing three types of nano particles namely Ag(silver), TiO_2 (Titanium Oxide) and Cu(copper). The nano particles are assumed to have a uniform shape and size. Moreover, It is assumed that both the fluid phase nanoparticles are in thermal equilibrium state. Due to semi-infinite plate surface assumption, further more the flow variables are functions of y and t only.

$v' = -V_0$, where the constant $-V_0$ represents the normal velocity at the plate which is positive suction ($V_0 > 0$) and negative for blowing injection ($V_0 < 0$).

Under the above boundary layer approximations, the governing equations for the nanofluid flow are given by

$$\frac{\partial v'}{\partial y'} = 0 \quad (1)$$

$$\frac{\partial u'}{\partial t'} + v' \frac{\partial u'}{\partial y'} = \frac{\mu_{nf}}{\rho_{nf}} \frac{\partial^2 u'}{\partial y'^2} + \frac{(\rho\beta)_{nf}}{\rho_{nf}} g(T' - T'_\infty) - \frac{\mu_{nf}}{\rho_{nf}} \frac{u'}{K'} - \frac{1}{\rho_{nf}} \sigma B_0^2 u' \quad (2)$$

$$\begin{aligned} (\rho C_p)_{nf} \left(\frac{\partial T'}{\partial t'} + v' \frac{\partial T'}{\partial y'} \right) &= \alpha_{nf} (\rho C_p)_{nf} \frac{\partial^2 T'}{\partial y'^2} - Q'(T' - T'_\infty) + Q_l (\rho C_p)_{nf} (C' - C'_\infty) \\ &\quad + \frac{D_m K_T}{C_s} \frac{\partial^2 C'}{\partial y'^2} \end{aligned} \quad (3)$$

$$\frac{\partial C'}{\partial t'} + v' \frac{\partial C'}{\partial y'} = D_B \frac{\partial^2 C'}{\partial y'^2} - K_l (C' - C'_\infty) \quad (4)$$

The relevant boundary conditions for the problem are given by

$$\begin{aligned} t' < 0, \quad u'(y', t') &= 0, \quad T' = T'_\infty, \quad C' = C'_\infty \\ t' \geq 0, \quad u'(y', t') &= U_0, \quad T' = T'_w + \varepsilon e^{\beta w' t'} (T'_w - T'_\infty), \\ C' &= C'_w + \varepsilon e^{\beta w' t'} (C'_w - C'_\infty) \quad \text{at } y' = 0 \\ u'(y', t') &= 0, \quad T' = T'_\infty, \quad C' = C'_\infty \quad \text{as } y' \rightarrow \infty \end{aligned} \quad (5)$$

The dimension less parameters feature in Equations (1) – (5) and are defined as:

$$\text{Pr} = \frac{\nu_f}{\alpha_f} \quad (\text{Prandtl number});$$

$$K = \frac{K' \rho_f U_0^2}{\nu_f^2 \mu_{nf}} \quad (\text{permeability parameter});$$

$$S = \frac{V_0}{U_0} \quad (\text{the suction}(S > 0) \text{ or injection}(S < 0) \text{ parameter});$$

$$M = \frac{\sigma B_0^2 \nu_f}{\rho_f U_0^2} \quad (\text{Magnetic parameter});$$

$$Sc = \frac{\nu_f}{D_B} \quad (\text{Schmidt number});$$

$$Gr = \frac{(\rho\beta)_f g v_f (T'_w - T'_\infty)}{\rho_f U_0^2} \text{ (Grashof number);}$$

$$Du = \frac{D_m K_T (C'_w - C'_\infty)}{k_f C_s (T'_w - T'_\infty)} \text{ (Diffusion-thermo parameter);}$$

$$u = \frac{u'}{U_0} \text{ (dimensional velocity component);}$$

$$y = \frac{U_0 y'}{v_f} \text{ (normal coordinate);}$$

$$t = \frac{U_0^2 t'}{v_f} \text{ (dimensional time);}$$

$$\theta = \frac{(T' - T'_\infty)}{(T'_w - T'_\infty)} \text{ (dimensionless temperature),}$$

$$Q_L = \frac{Q'_l (C'_w - C'_\infty)}{U_0^2 (T'_w - T'_\infty)} \text{ (radiation absorption parameter);}$$

$$Kr = \frac{K_l v_f}{U_0^2} \text{ (Chemical reaction parameter);}$$

$$\psi = \frac{(C' - C'_\infty)}{(C'_w - C'_\infty)} \text{ (dimensionless concentration);}$$

$$\mu_{nf} = \rho_f v_f \text{ (viscosity of nanofluid).}$$

In equations (2) – (4) with the boundary conditions (5) we obtain

$$\frac{\partial u}{\partial t} - S \frac{\partial u}{\partial y} = \frac{D}{A} \frac{\partial^2 u}{\partial y^2} + \frac{B}{A} Gr \theta - \left(M + \frac{1}{K} \right) u \tag{6}$$

$$\frac{\partial \theta}{\partial t} - S \frac{\partial \theta}{\partial y} - Q_L \psi = \frac{1}{C Pr} \left(E \frac{\partial^2 \theta}{\partial y^2} - Q \theta \right) + \frac{Du}{C Pr} \frac{\partial^2 \psi}{\partial y^2} \tag{7}$$

$$Sc \frac{\partial \psi}{\partial t} - Sc S \frac{\partial \psi}{\partial y} = \frac{\partial^2 \psi}{\partial y^2} - Sc Kr \psi \tag{8}$$

The corresponding boundary conditions are

$$\begin{aligned}
 t < 0: u = 0, \theta = 0, \psi = 0 \\
 t \geq 0: u = 1, \theta = 1 + \varepsilon e^{i\omega t}, \psi = 1 + \varepsilon e^{i\omega t} \quad \text{at } y = 0 \\
 u = 0, \theta = 0, \psi = 0 \quad \text{as } y \rightarrow \infty
 \end{aligned} \tag{9}$$

3. NUMERICAL SOLUTIONS BY TWO TERM PERTURBATION TECHNIQUE

Equations (6) – (8) are coupled non-linear partial differential equations whose solutions in closed-form are difficult to obtain. To solve these equations by converting into ordinary differential equations, the unsteady flow is superimposed on the mean steady flow, so that in the neighborhood of the plate, the expressions for velocity, temperature and concentration are assumed as

$$u(y) = u_0(y) + \varepsilon e^{i\omega t} u_1(y) + O(\varepsilon^2) \tag{10}$$

$$\theta(y) = \theta_0(y) + \varepsilon e^{i\omega t} \theta_1(y) + O(\varepsilon^2) \tag{11}$$

$$\psi(y) = \psi_0(y) + \varepsilon e^{i\omega t} \psi_1(y) + O(\psi^2) \tag{12}$$

Where $\varepsilon \ll 1$ is a perturbation parameter.

Now substituting equations (10) – (12) into equations (6) – (8) and equating the harmonic and non-harmonic terms and neglecting higher order terms, using relevant boundary conditions, we obtain the expressions for velocity, temperature and concentration as

$$\begin{aligned}
 u(y,t) = (L_5 e^{-m_5 y} + L_3 e^{-m_3 y} + L_4 e^{-m_1 y}) \\
 + \varepsilon e^{i\omega t} (L_8 e^{-m_6 y} + L_6 e^{-m_4 y} + L_7 e^{-m_2 y})
 \end{aligned} \tag{13}$$

$$\theta(y,t) = (L_1 e^{-m_3 y} + A_1 e^{-m_1 y}) + \varepsilon e^{i\omega t} (L_2 e^{-m_4 y} + A_2 e^{-m_2 y}) \tag{14}$$

$$\psi(y,t) = e^{-m_1 y} + \varepsilon e^{i\omega t} e^{-m_2 y} \tag{15}$$

The dimensionless skin-friction coefficient, rate of heat transfer and rate of mass

transfer are given by

$$\tau = -\left(\frac{\partial u}{\partial y}\right)_{y=0} = (L_5 m_5 + L_3 m_3 + L_4 m_1) + \varepsilon e^{i\omega t} (L_8 m_6 + L_6 m_4 + L_7 m_2) \tag{16}$$

$$Nu = -\left(\frac{\partial \theta}{\partial y}\right)_{y=0} = (L_1 m_3 + A_1 m_1) + \varepsilon e^{i\omega t} (L_2 m_4 + A_2 m_2) \tag{17}$$

$$Sh = -\left(\frac{\partial \psi}{\partial y}\right)_{y=0} = m_1 + \varepsilon e^{i\omega t} m_2 \tag{18}$$

4. RESULTS AND DISCUSSIONS

In order to bring out the silent features of the flow, heat and mass transfer characteristics with nanoparticles, the results are presented in Figures 2-10 and Tables 1-3. The influences of nanoparticles on the velocity, the temperature and the concentration distributions as well as on the skin-friction, the heat transfer rate and mass transfer rate are discussed numerically. We have assumed here $\varepsilon = 0.02$, $t = 1$, $\omega = 1$ and $Pr = 0.71$, while the remaining parameters are varied over a range.

4.1. Variations of the Velocity Distribution and skin-friction coefficient

Figure 2(a), 2(b) and 2(c) demonstrates the effect of suction parameter S on fluid velocity u for both regular ($\phi = 0$) and nano fluid ($\phi \neq 0$). As out put of figures, it is seen that the velocity of the fluid across the boundary layer by increasing the suction parameter S for both regular and nano fluid with Nano particles Ag, TiO_2 and Cu. It is worth mentioned here that the influence of the suction parameter S on the fluid velocity is more effective for TiO_2 water nanofluid than that of Ag water nanofluid and Cu water nanofluid. Figure 3(a), 3(b) and 3(c) witnessed the influence of radiation absorption parameter Q_L on velocity distribution. It is clear from the figures that velocity increase with increase of Q_L . The magnetic parameter M on velocity profiles for Nano particles Ag, TiO_2 and Cu are shown in figures 4(a), 4(b) and 4(c). From these graphs, it is obvious that nanofluid velocity of the fluid decelerates with an increase in the strength of magnetic field. The influences of a transverse magnetic field on an electrically, conducting fluid give rise to a resistive-type force called the Lorentz force. This force has the tendency to slow down the motion of the fluid in the boundary layer. Also it is clear that the nanofluid velocity is lower for the regular fluid. The numerical values of the skin-friction coefficient for the nanoparticles Ag,

TiO₂ and Cu are in Table 1. From this table, it is seen that the skin-friction coefficient increases with increase values of S, Du, M, Q_L, Pr while decrease with increase values of Sc and K for the three nanoparticles Ag, TiO₂ and Cu.

4.2. Variations of the Temperature Distribution and heat transfer rate

The influence of Diffusion Thermo parameter Du on the temperature distribution for Ag water, TiO₂ water and Cu water nano fluids is portrayed in figures 5(a), 5(b) and 5(c) with in boundary layer. With the increasing values of Du, the temperature of nanofluid is found to increase the thermal boundary layer thickness. The graphical representation of prandtl number Pr on temperature profiles as depicted in figures 6(a), 6(b) and 6(c) with in boundary layer. It is observed that the growing Pr increases the temperature boundary layer. Table 2. denotes the numerical values of heat transfer rate for different fluid flow parameters Du, ϕ , Q_L and Q for Ag water, TiO₂ water and Cu water nano fluids. From this table it is clear that the heat transfer rate increases with ϕ and Q, while decreases with Du and Q_L.

4.3. Variations of the Concentration Distribution and mass transfer rate

Figure 7. displays the effects of the perturbation parameter ε on the species concentration profiles. As perturbation parameter increases the species concentration decreases. For different values of destructive chemical reaction parameter Kr the concentration profiles are plotted in Figure 8. An increase in chemical reaction parameter will suppress the concentration of the fluid. The concentration distribution decreases at all points of the flow field with the increase in the chemical reaction parameter. Figure 9. Portrays the influences of Schmidt number for various values. As Sc is increase, concentration is decrease. The effects of the suction parameter S on the species concentration was depicted in Figure 10. As S increases, the solutal boundary layer thickness increases. This is due to the usual fact that the suction stabilizes the boundary growth. These consequences are obviously supported from the physical point of view. From Table 3. ,it is seen that the local Sherwood number increases with increasing values of Schmidt Sc, suction parameter S and chemical reaction parameter Kr.

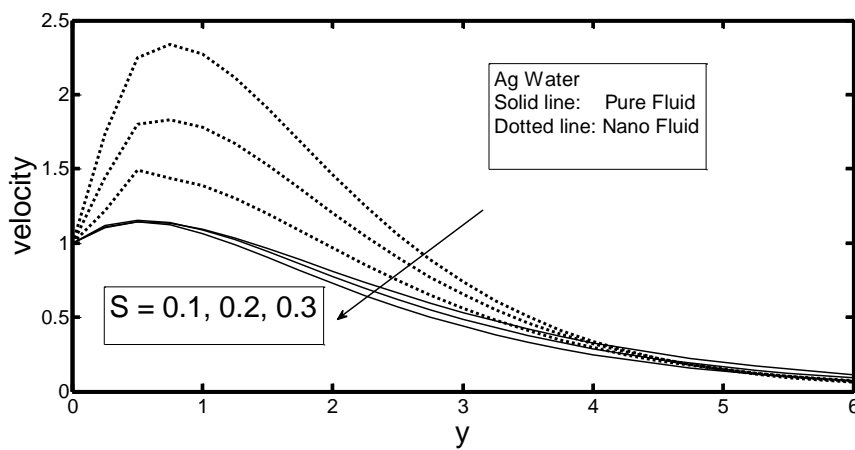


Figure 2(a). Plot of suction parameter(S) on velocity profile with Ag-water.

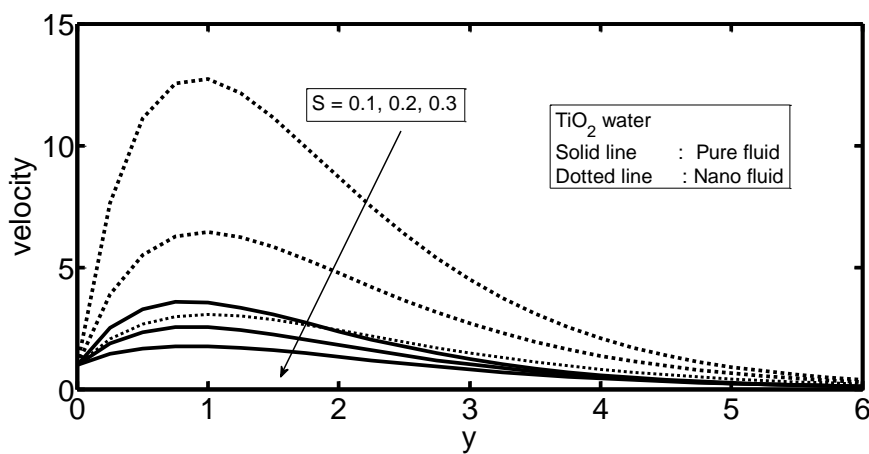


Figure 2(b). Plot of suction parameter(S) on velocity profile with TiO₂-water.

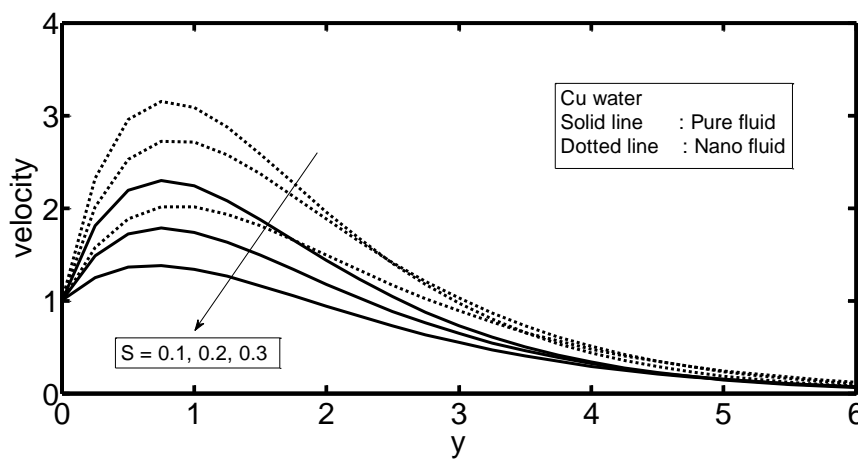


Figure 2(c). Plot of suction parameter(S) on velocity profile with Cu-water.

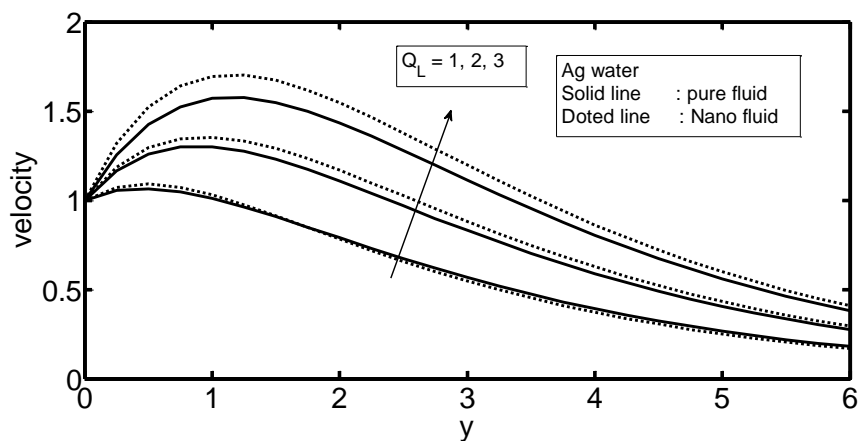


Figure 3(a). Plot of radiation absorption parameter(Q_L) on velocity profile with Ag-water.

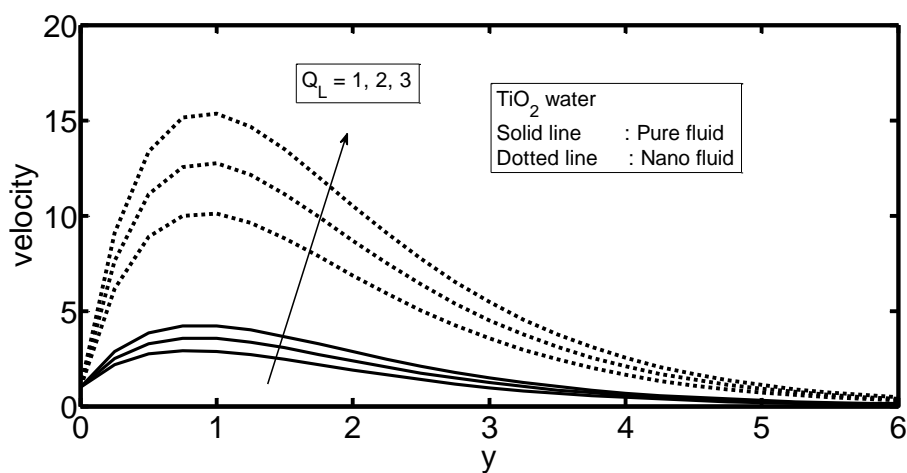


Figure 3(b). Plot of radiation absorption parameter(Q_L) on velocity profile with TiO_2 -water.

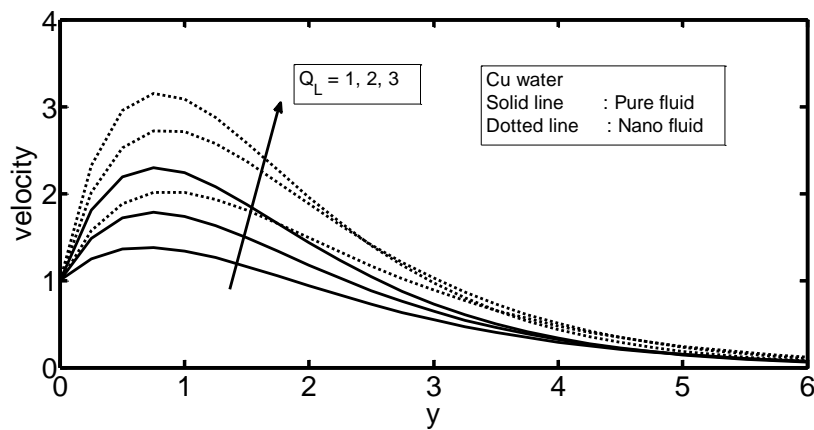


Figure 3(c). Plot of radiation absorption parameter(Q_L) on velocity profile with Cu-water.

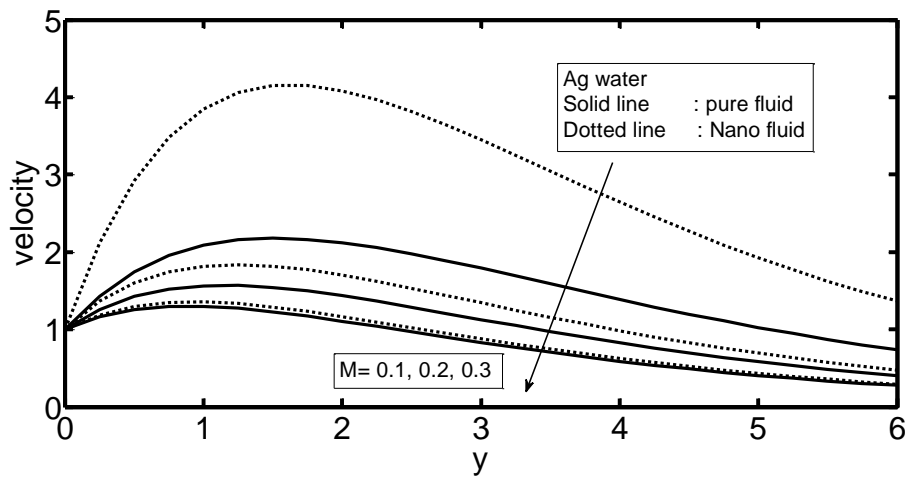


Figure 4(a). Plot of magnetic parameter(M) on velocity profile with Ag-water.

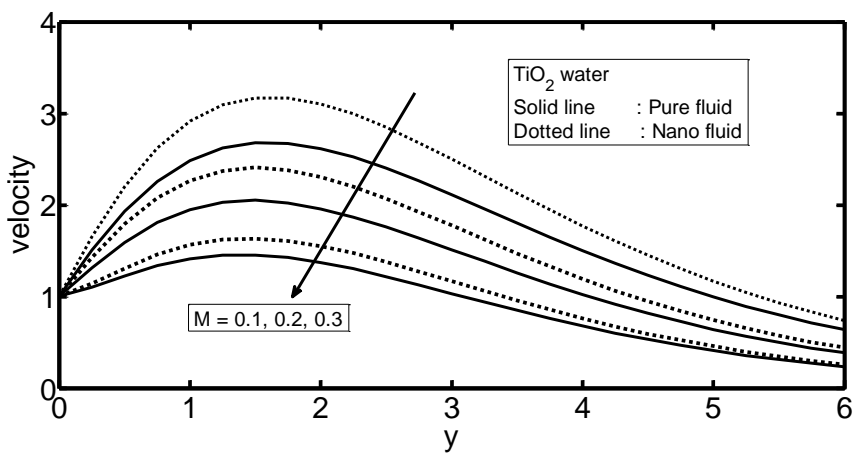


Figure 4(b). Plot of magnetic parameter(M) on velocity profile with TiO₂-water.

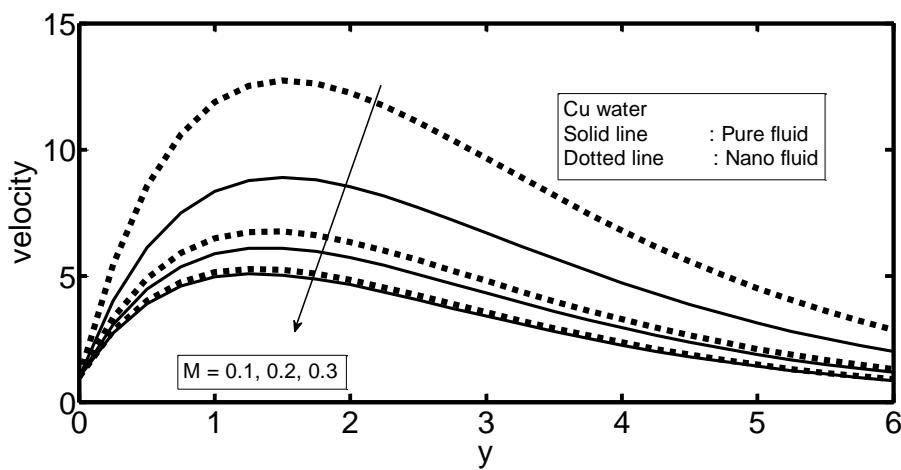
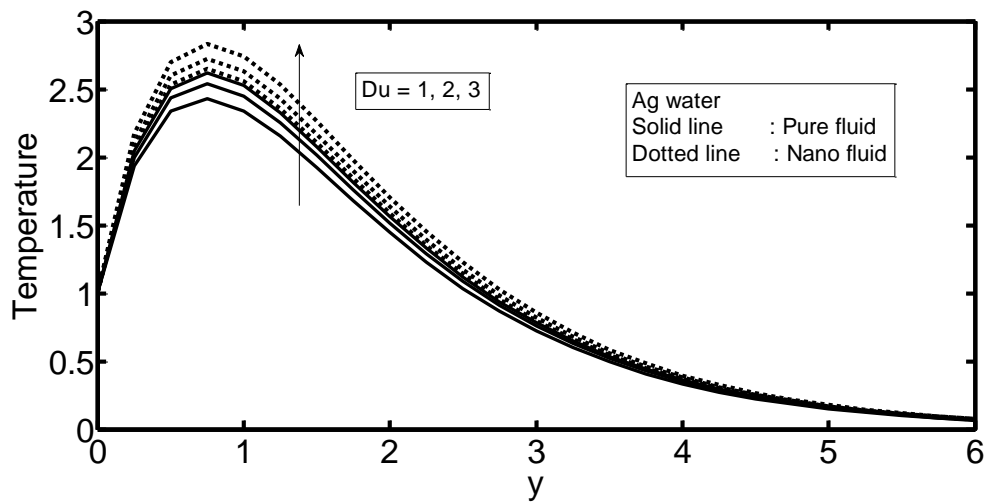


Figure 4(c). Plot of magnetic parameter(M) on velocity profile with Cu-water.

Table 1. Comparison of skin-friction coefficient values among Ag, Alu and Cu with $\phi = 0.25$.

| S | Du | M | QL | Sc | Pr | K | Ag | TiO ₂ | Cu |
|------------|------------|------------|------------|----------|----------|------------|--------|------------------|--------|
| 0.1 | 0.5 | 0.5 | 2 | 0.60 | 0.71 | 4 | 1.6936 | 0.6809 | 1.3538 |
| 0.2 | 0.5 | 0.5 | 2 | 0.60 | 0.71 | 4 | 4.7874 | 1.3158 | 3.3558 |
| 0.3 | 0.5 | 0.5 | 2 | 0.60 | 0.71 | 4 | 8.2813 | 1.9359 | 6.5938 |
| 0.1 | 0.2 | 0.5 | 2 | 0.60 | 0.71 | 4 | 1.5584 | 0.6537 | 1.2561 |
| 0.1 | 0.3 | 0.5 | 2 | 0.60 | 0.71 | 4 | 1.6034 | 0.6628 | 1.2885 |
| 0.1 | 0.4 | 0.5 | 2 | 0.60 | 0.71 | 4 | 1.6485 | 0.6718 | 1.3209 |
| 0.1 | 0.5 | 0.1 | 2 | 0.60 | 0.71 | 4 | 0.6144 | 0.1763 | 0.4816 |
| 0.1 | 0.5 | 0.2 | 2 | 0.60 | 0.71 | 4 | 0.8186 | 0.2975 | 0.6576 |
| 0.1 | 0.5 | 0.3 | 2 | 0.60 | 0.71 | 4 | 1.0463 | 0.4165 | 0.8473 |
| 0.1 | 0.5 | 0.5 | 0.1 | 0.60 | 0.71 | 4 | 0.8887 | 0.5195 | 0.7746 |
| 0.1 | 0.5 | 0.5 | 0.2 | 0.60 | 0.71 | 4 | 0.9311 | 0.5280 | 0.8050 |
| 0.1 | 0.5 | 0.5 | 0.3 | 0.60 | 0.71 | 4 | 0.9735 | 0.5365 | 0.8355 |
| 0.1 | 0.5 | 0.5 | 2 | 1 | 0.71 | 4 | 0.8486 | 0.4557 | 0.7325 |
| 0.1 | 0.5 | 0.5 | 2 | 2 | 0.71 | 4 | 0.6081 | 0.3771 | 0.5451 |
| 0.1 | 0.5 | 0.5 | 2 | 3 | 0.71 | 4 | 0.5837 | 0.3769 | 0.5285 |
| 0.1 | 0.5 | 0.5 | 2 | 0.60 | 1 | 4 | 2.0172 | 0.7443 | 1.5856 |
| 0.1 | 0.5 | 0.5 | 2 | 0.60 | 2 | 4 | 3.0582 | 0.9353 | 2.3285 |
| 0.1 | 0.5 | 0.5 | 2 | 0.60 | 3 | 4 | 3.9885 | 1.0873 | 2.9864 |
| 0.1 | 0.5 | 0.5 | 2 | 0.60 | 0.71 | 0.2 | 1.4822 | 1.4566 | 1.4830 |
| 0.1 | 0.5 | 0.5 | 2 | 0.60 | 0.71 | 0.4 | 0.5769 | 0.7825 | 0.6473 |
| 0.1 | 0.5 | 0.5 | 2 | 0.60 | 0.71 | 0.6 | 0.1128 | 0.4228 | 0.2086 |

**Figure 5(a).** Plot of Dufour number(Du) on temperature profile with Ag-water.

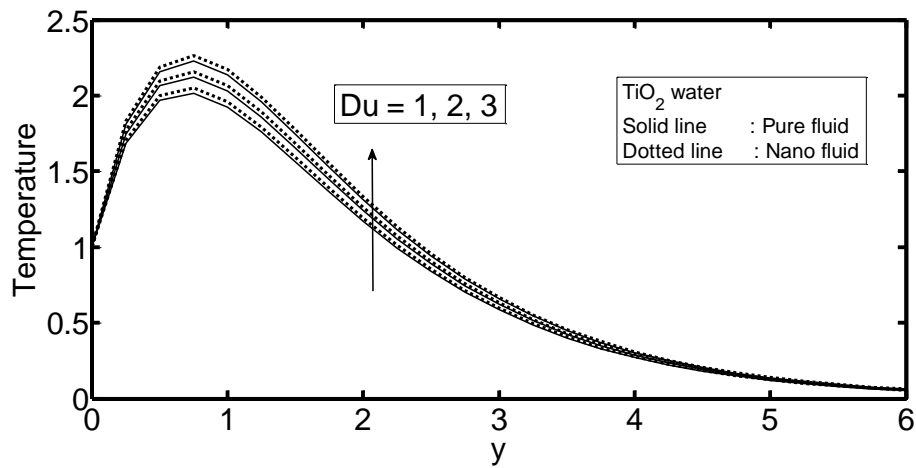


Figure 5(b). Plot of Dufour number(Du) on temperature profile with TiO₂-water.

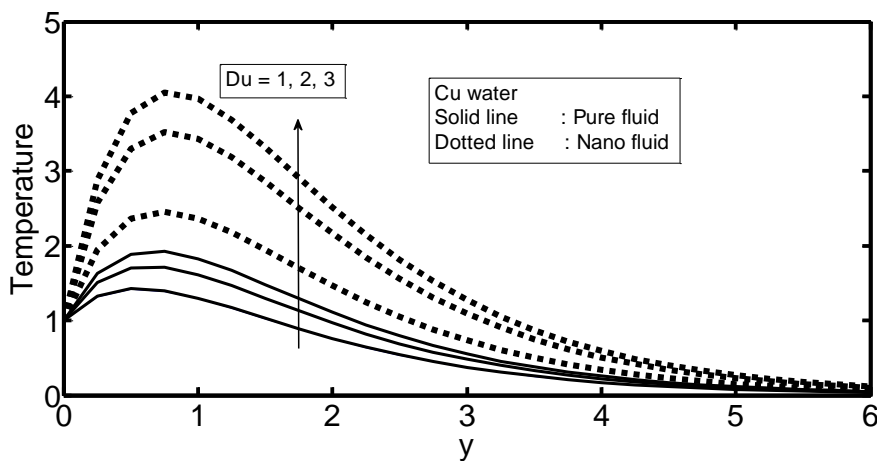


Figure 5(c). Plot of Dufour number(Du) on temperature profile with Cu-water.

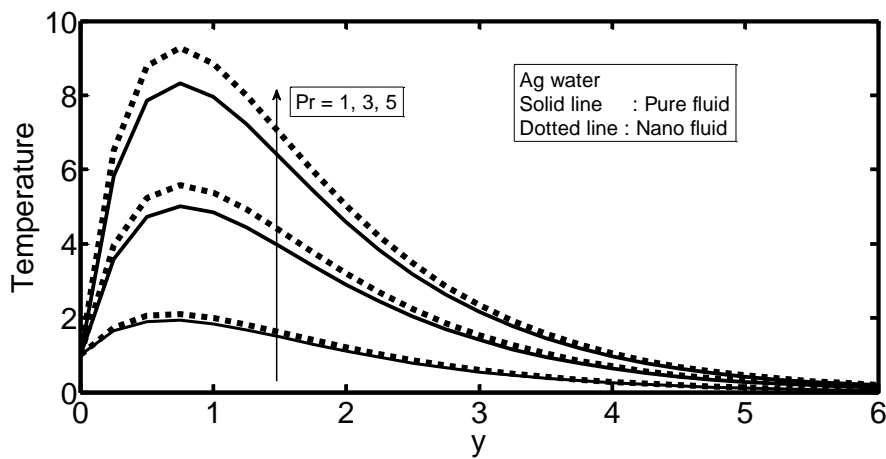


Figure 6(a). Plot of Prandtl number(Pr) on temperature profile with Ag-water.

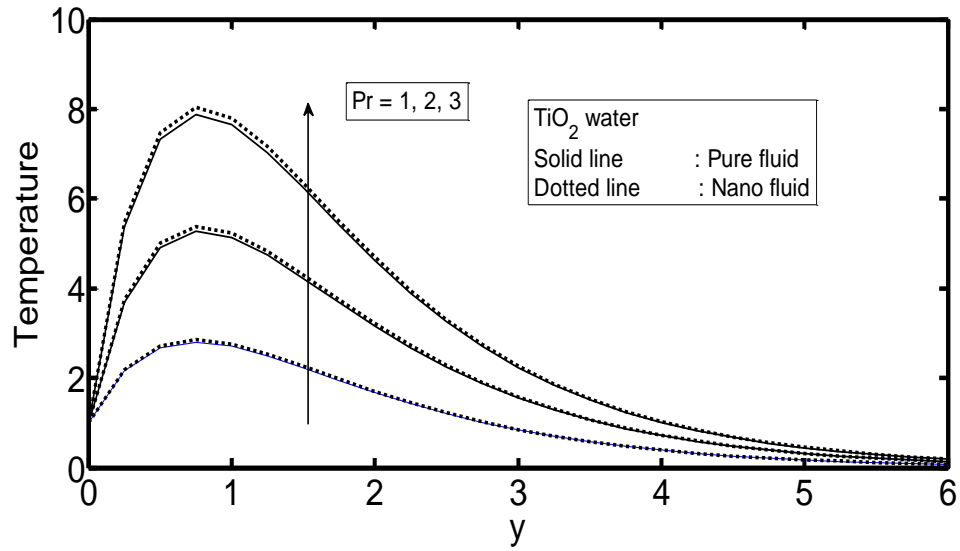


Figure 6(b). Plot of Prandtl number(Pr) on temperature profile with TiO₂-water.

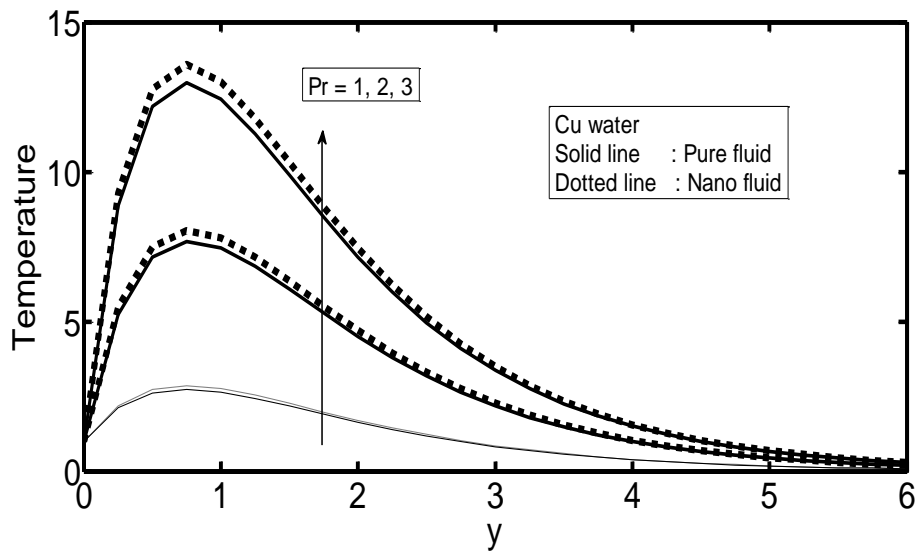


Figure 6(c). Plot of Prandtl number(Pr) on temperature profile with Cu-water.

Table 2. Comparison of rate of heat transfer values among Ag, Alu and Cu with $\phi = 0.25$.

| Du | ϕ | QL | Q | Ag | TiO ₂ | Cu |
|------------|-------------|----------|----------|--------|------------------|--------|
| 0.2 | 0.25 | 2 | 0.60 | 1.1206 | 1.0795 | 1.0908 |
| 0.3 | 0.25 | 2 | 0.60 | 1.0872 | 1.0660 | 1.0773 |
| 0.4 | 0.25 | 2 | 0.60 | 1.0538 | 1.0526 | 1.0638 |
| 0.5 | 0.05 | 2 | 0.60 | 0.9957 | 1.0391 | 1.0383 |
| 0.5 | 0.10 | 2 | 0.60 | 1.0019 | 1.0430 | 1.0413 |
| 0.5 | 0.15 | 2 | 0.60 | 1.0081 | 1.0469 | 1.0443 |
| 0.5 | 0.20 | 2 | 0.60 | 1.0142 | 1.0508 | 1.0474 |
| 0.5 | 0.5 | 2 | 0.60 | 0.7151 | 0.6945 | 0.6712 |
| 0.5 | 0.5 | 3 | 0.60 | 0.4099 | 0.3341 | 0.2920 |
| 0.5 | 0.5 | 4 | 0.60 | 0.1047 | 0.0262 | 0.0872 |
| 0.5 | 0.5 | 2 | 3 | 1.4073 | 1.4369 | 1.4393 |
| 0.5 | 0.5 | 2 | 4 | 1.7194 | 1.7454 | 1.7526 |
| 0.5 | 0.5 | 2 | 5 | 1.9875 | 2.0104 | 2.0212 |

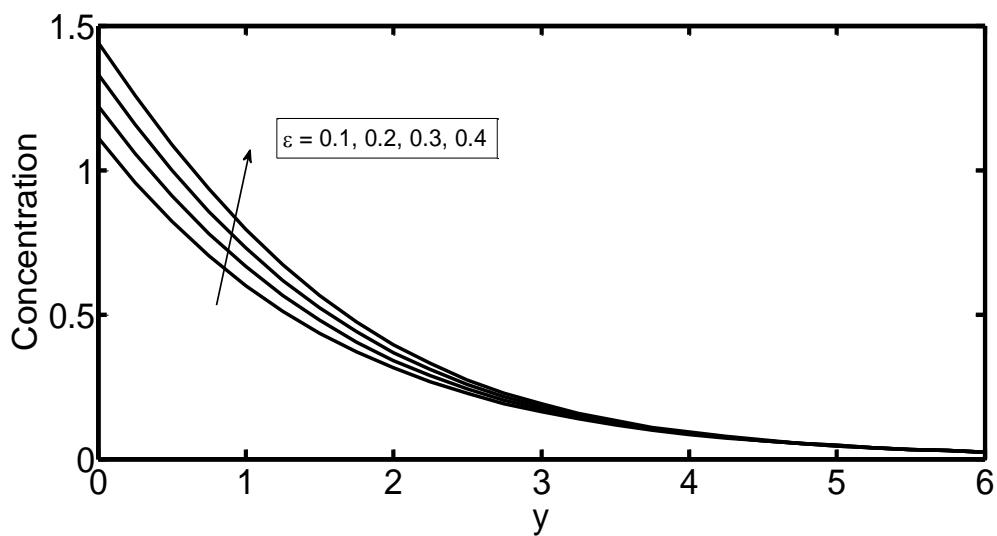


Figure7. Plot of Perturbation parameter(ϵ) on concentration profile with different values.

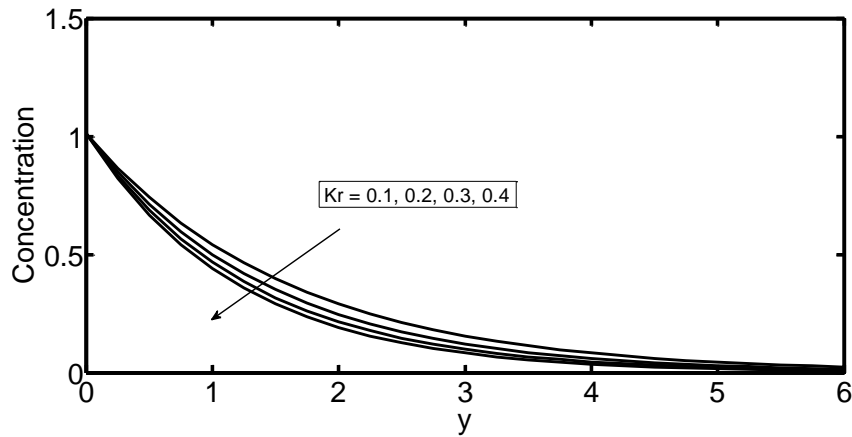


Figure 8. Plot of Chemical reaction parameter(Kr) on concentration profile with different values.

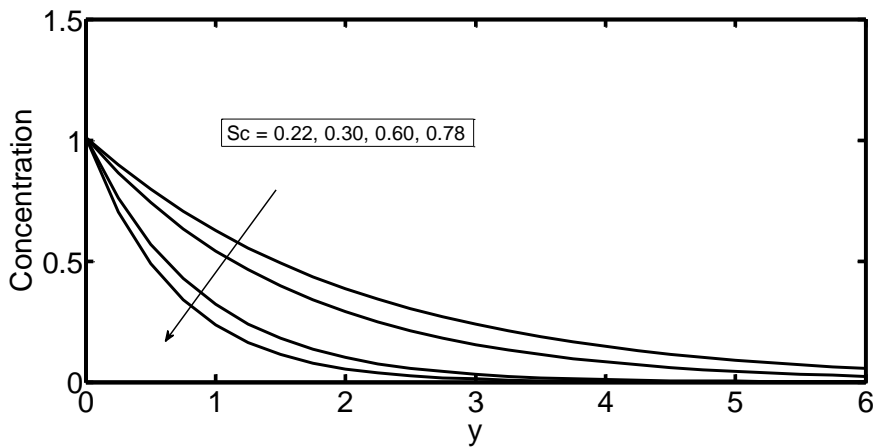


Figure 9. Plot of Schmidt number(Sc) on concentration profile with different values.

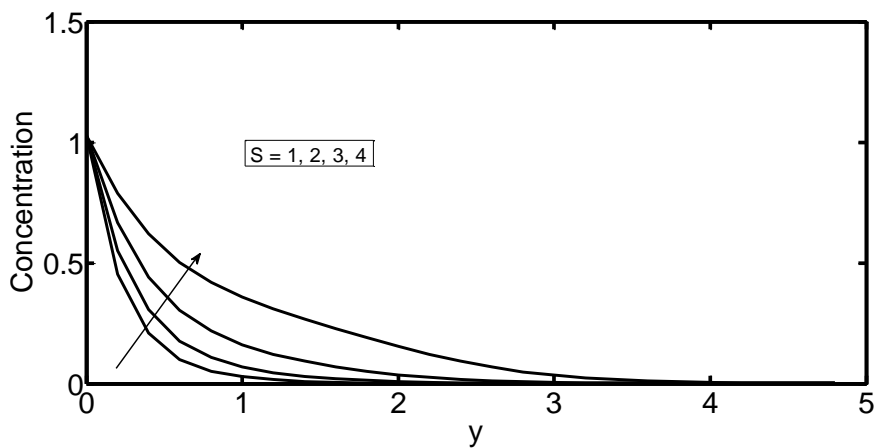


Figure 10. Plot of Suction parameter(S) on concentration profile with different values.

Table3.Numerical values for rate of mass transfer.

| Sc | S | Kr | Sh |
|-------------|------------|------------|--------|
| 0.22 | 0.1 | 0.5 | 0.4962 |
| 0.30 | 0.1 | 0.5 | 0.5839 |
| 0.60 | 0.1 | 0.5 | 0.8440 |
| 0.78 | 0.1 | 0.5 | 0.9724 |
| 0.1 | 0.2 | 0.5 | 0.9081 |
| 0.1 | 0.3 | 0.5 | 0.9745 |
| 0.1 | 0.4 | 0.5 | 1.0432 |
| 0.1 | 0.5 | 0.5 | 1.1141 |
| 0.1 | 0.1 | 0.1 | 0.4132 |
| 0.1 | 0.1 | 0.2 | 0.5572 |
| 0.1 | 0.1 | 0.3 | 0.6681 |
| 0.1 | 0.1 | 0.4 | 0.7616 |

Table 4. Thermo physical properties of fluid and nanoparticles given by Oztop and Abu-Nada[21].

| Physical properties | water | Cu | Al ₂ O ₃ | TiO ₂ | Ag |
|------------------------|-------|------|--------------------------------|------------------|-------|
| C _p (J/kgK) | 4179 | 385 | 765 | 686.2 | 235 |
| ρ(kg/m ³) | 997.1 | 8933 | 3970 | 4250 | 10500 |
| k(W/mK) | 0.613 | 400 | 40 | 8.9538 | 429 |
| βX10 ⁻⁵ | 21 | 1.67 | 0.85 | 0.9 | 1.89 |

CONCLUSIONS

We have performed Analysis of Heat and Mass Transfer on MHD flow with Ag, Al₂O₃ and Cu Water Nanofluids over a Semi Infinite Flat Surface. In this article we considered Ag-water, TiO₂-water and Cu-water nanofluids. We have solved the model equations using perturbation technique. The following conclusions can be made from the present investigation.

- The silver(Ag) nanoparticles proved to have the maximum cooling recital for this vertical porous plate problem where Alumina nanoparticles have the lowest. This is due to the high thermal conductivity of Ag and low thermal conductivity of TiO₂ and Cu.
- The velocity profile increases with an increase in radiation absorption parameter.
- The temperature profile increases with an increase in Dufour number.

- Due to chemical reaction, the concentration of the fluid decreases. This is because the consumption of chemical species leads to fall in the species concentration field.

We hope that the findings of this investigation may be useful in catalysis, biomedicine, magnetic resonance imaging, data storage and environmental remediation. Hence, the subject of nanofluids is of great interest worldwide for basic and applied research.

REFERENCES

- [1] R.V.M.S.S Kiran kumar, P.Durga Prasad, S.V.K.Varma, “analytical study of heat and mass transfer enhancement in free convection flow with chemical reaction and constant heat source in nano-fluids”, *Procedia Engineering*,127(2015):978-985.
- [2] G.Venkataramanaiah, M.Sreedhar Babu, M.Lavanya, “heat generation / absorption effects on magneto-williamson nano fluid flow with heat and mass fluxes”, *international journal of engineering development and research*, 4(2016):384-397.
- [3] Dodda Ramya, R.Srinivasa raju, J.Anandrao, M.M.Rashidi, “boundary layer viscous flow of nanofluids and heat transfer over a nonlinearly isothermal stretching sheet in the presence of heat generation/absorption and slip boundary conditions”, *Int.J.Nanosci.Nanotechnol.*,12(2016):251-268.
- [4] P.Srinivasulu, T.Poornima, N. Baskar reddy, “influence of magnetic field and viscous dissipation on nanofluids past a nonlinear stretching sheet with radiation and uniform heat source”, *Proceedings of International Conference on Frontiers in Mathematics(2015)*, March 26-28, Gauhati University, Guwahati, Assam, India.
- [5] Fekry M Hady, Fouad S Ibrahim, Sahar M Abdel-Gaied, Mohamed R Eid, “radiation effect on viscous flow of nano-fluid and heat transfer over a nonlinearly stretching sheet”, *Nanoscale Research Letters*, Springer, 7(2012):1-13.
- [6] Sandeep Naramgiri, C.Sulochana, “dual solutions for MHD stagnation point flow of a nano fluid over stretching surface with induced magnetic field”, *International Journal of Science and Engineering*, 9(2015):1-8.
- [7] Nader Y Abd Elazem, Abdelhalim Ebaid, Emad H Aly, “radiation effect of MHD on cu-water and ag-water Nanofluids flow over a Stretching Sheet: Numerical study”, *J.Applied and Computational Mathematics*, 4(2015):1-8.
- [8] Nageeb A Haroun, Precious Sibanda, Sabyasachi Mondal, Sandile S Motsa, “On unsteady MHD mixed convection in a nano-fluid due to a stretching/shrinking surface with suction/injection using the spectral relaxation method”, *Boundary values problems*, springer, 24(2015):1-17.
- [9] Eshetu Haile, B.Shankar, “boundary-layer flow of nanofluids over a moving

- surface in the presence of thermal radiation, viscous dissipation and chemical reaction”, *Applications and Applied Mathematics*,10(2015):952-969.
- [10] P.V.Satyanarayana, B.Venkateswarulu, “heat and mass transfer on mhd nano fluid flow past a vertical porous plate in a rotating system”, *Frontiers in Heat and Mass Transfer*,7(2016):1-10.
- [11] Mohammad Mehdi Keshtekar, Ahmad Khaluei, Hadi Ameri Fard, “effects of thermal radiation, viscous dissipation, variable magnetic field and suction on mixed convection MHD flow of nano fluid over a nonlinear stretching sheet”, *IOSR journal of Engineering*, 04(2014):44-54.
- [12] M.J.Uddin, A.Sohail, O.Anwer Beg, “numerical solution of MHD slip flow of a nanofluid past a radiating plate with Newtonian heating: a lie group approach”, *Alexandria Engineering Journal*, March 4th 2017(accepted).
- [13] Mohamed Abdel-wahed, Tarek Emam, “mhd boundary layer behavior over a moving surface in a nanofluid under the influence of convective boundary conditions”, *Journal of Mechanical Engineering*, 63(2017):119-128.
- [14] K.Vendabai, G.Sarojamma, “unsteady convective boundary layer of a nano fluid over a stretching surface in the presence of a magnetic field and heat generation”, *International Journal of Emerging Trends in Engineering and Development*, 4(2014):214-230.
- [15] D.R.V.S.R.Sastry, “MHD thermosolutal marangoni convection boundary layer nano fluid flow past a flat plate with radiation and chemical reaction”, *Indian Journal of science and technology*, 8(2015):1-8.
- [16] S.A.Shehzad, T.Hayat, A.Alsaedi, “influence of convective heat and mass conditions in MHD FLOW OF nanofluid”, *Bulletin of the Polish Academy Of Sciences*, 63(2015):465-474.
- [17] Imran Anwar, Abdul Rahman Mohd Kasim, Zulkibri Ismail, Mohd Zuki Salleh, Sharidan Shafie, “chemical reaction and uniform heat generation of absorption effects on mhd stagnation-point flow of a nanofluid over a porous sheet”, *World Applied Sciences Journal*, 24(2013):1390-1398.
- [18] M.Turkyilmazoglu, “natural convective flow of nanofluids past a radiative and impulsive vertical plate”, *J.Aerosp. Eng.*, 29(2016):1-8.
- [19] G.S.Seth, S.M.Hussain, S.Sarkar, “effects of hall current and rotation on unsteady MHD natural convection flow with heat and mass transfer past an impulsively moving vertical plate in the presence of radiation and chemical reaction”, 46(2014):704-718.
- [20] Wubshet Ibrahim, Bandari Shankar, “MHD boundary layer flow and heat transfer of a nanofluid past a permeable stretching sheet with velocity, thermal and solutol slip boundary conditions”, 75(2013):1-10.
- [21] Oztop.H.F. and E.Abu-Nada, “Numerical study of natural convection in partially heated rectangular enclosures filled with nanofluid”, *Int.J.Heat Fluid Flow*,29(2008):1326-1336.

APPENDIX

$$\rho_{nf} = (1-\phi)\rho_f + \phi\rho_s;$$

$$(\rho C_p)_{nf} = (1-\phi)(\rho C_p)_f + \phi(\rho C_p)_s;$$

$$(\rho\beta)_{nf} = (1-\phi)(\rho\beta)_f + \phi(\rho\beta)_s;$$

$$K_{nf} = K_f \left(\frac{K_s + 2K_f - 2\phi(K_f - K_s)}{K_s + 2K_f + 2\phi(K_f - K_s)} \right);$$

$$\mu_{nf} = \frac{\mu_f}{(1-\phi)^{2.5}};$$

$$\alpha_{nf} = \frac{K_{nf}}{(\rho C_p)_{nf}};$$

$$A = \left((1-\phi) + \phi \left(\frac{\rho_s}{\rho_f} \right) \right);$$

$$B = \left((1-\phi) + \phi \left(\frac{(\rho\beta)_s}{(\rho\beta)_f} \right) \right);$$

$$C = \left((1-\phi) + \phi \left(\frac{(\rho C_p)_s}{(\rho C_p)_f} \right) \right);$$

$$D = \frac{1}{(1-\phi)^{2.5}};$$

$$E = \frac{K_{nf}}{K_f} = \left(\frac{(1+2\phi) + 2(1-\phi) \left(\frac{K_f}{K_s} \right)}{(1+2\phi) + 2(1+\phi) \left(\frac{K_f}{K_s} \right)} \right);$$

$$m_1 = \left(\frac{SSc + \sqrt{(SSc)^2 + 4KrSc}}{2} \right);$$

$$m_2 = \left(\frac{SSc + \sqrt{(SSc)^2 + 4Sc(i\omega + Kr)}}{2} \right);$$

$$m_3 = \left(\frac{\text{Pr } CS + \sqrt{(\text{Pr } CS)^2 + 4EQ}}{2} \right);$$

$$m_4 = \left(\frac{\text{Pr } SC + \sqrt{4E(Q + i\omega \text{Pr } C)}}{2E} \right);$$

$$m_5 = \left(\frac{AS + \sqrt{(AS)^2 + 4D \left(M + \frac{1}{K} \right)}}{2D} \right);$$

$$m_6 = \left(\frac{AS + \sqrt{(AS)^2 + 4D \left(Ai\omega + \left(M + \frac{1}{K} \right) \right)}}{2D} \right);$$

$$L_1 = 1 - A_1;$$

$$L_2 = 1 - A_2;$$

$$L_3 = - \left(\frac{BL_1 Gr}{Dm_3^2 - ASm_3 - \left(M + \frac{1}{K} \right)} \right);$$

$$L_4 = - \left(\frac{BA_1 Gr}{Dm_1^2 - ASm_1 - \left(M + \frac{1}{K} \right)} \right);$$

$$L_5 = 1 - L_3 - L_4;$$

$$L_6 = - \left(\frac{BL_2 Gr}{Dm_4^2 - ASm_4 - \left(Ai\omega + M + \frac{1}{K} \right)} \right);$$

$$L_7 = - \left(\frac{BGrA_2}{Dm_2^2 - ASm_2 - \left(Ai\omega + M + \frac{1}{K} \right)} \right);$$

$$L_8 = -B_6 - B_7;$$

$$A_1 = - \left(\frac{m_1^2 Du + Pr Q_L C}{Em_1^2 - Pr CSm_1 - Q} \right);$$

$$A_2 = \left(\frac{m_2^2 Du + C Pr Q_L}{Em_2^2 - C Pr m_2 - (Q + i\omega C Pr)} \right).$$